Subdivision Directional Fields - Stencils

ACM Reference format:
. 2020. Subdivision Directional Fields - Stencils. 1, 1, Article 1 (June 2020), 3 pages.
https://doi.org/10.1145/nnnnnnn.nnnnnnn

In the following we details our subdivision stencils and the way we derived them. We modified the integrated face-based subdivision $S_{\mathcal{F}^*}$ operator, derived from the DEC S_2 in SEC [de Goes et al. 2016], to accommodate for our boundary conditions, and consequently had to modify S_1 around boundary vertices. In addition, we introduced a subdivision for unsigned integrated edge functions $S_{\mathcal{E}^*}$. We denote the number of incident faces as d, so that the regular interior stencils have $d = 6$ and the regular boundary stencils have $d = 3$. In addition, we denote boundary vertices by a black dot and an interior vertex by an open dot.

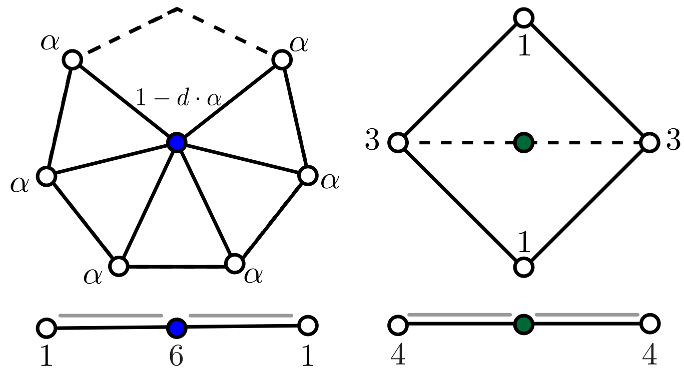

Fig. 1. Loop subdivision stencils used for $S_{\mathcal{V}}$ in our setting. The blue dot denotes even vertices (part of the original mesh), whereas the green dots denote the odd vertices (newly inserted in the subdivision step). Double edges denote boundary edges. Multiply all factors by 1/8, except for the α and $1 - d \cdot \alpha$ factors.

1 LOOP SUBDIVISION

For $S_{\mathcal{V}}$, we chose Loop subdivision (Fig. 1) with

$$\alpha = \begin{cases} \frac{3}{8d}, & d \neq 3 \\ \frac{3}{16}, & d = 3, \end{cases} \tag{1}$$

following Biermann et al. [2000]. The templates can be found in Figure 1. Similar to de Goes et al. [de Goes et al. 2016], we chose to keep the odd stencil next to the boundary the same as the interior stencil.

2 HALFBOX SPLINE SUBDIVISION

For the halfbox spline subdivision operator $S_{\mathcal{F}^*}$, we use the same stencils as Wang et al. [2006] for the interior faces, as given by Figure 2. Due to the extra constraints on $S_{\mathcal{E}^*}$ at the boundary, we modified the boundary stencils for $S_{\mathcal{F}}$. The parameters of the interior stencils are given by

$$\delta_1 = \frac{3}{4} - \beta \tag{2}$$

$$\delta_2 = \begin{cases} \frac{1}{8} & d > 3, \\ \frac{1}{8} + \frac{\beta}{2} & d = 3 \end{cases} \tag{3}$$

$$\delta_3 = \begin{cases} \frac{\beta}{2} & d > 4, \\ \beta & d = 4 \end{cases} \tag{4}$$

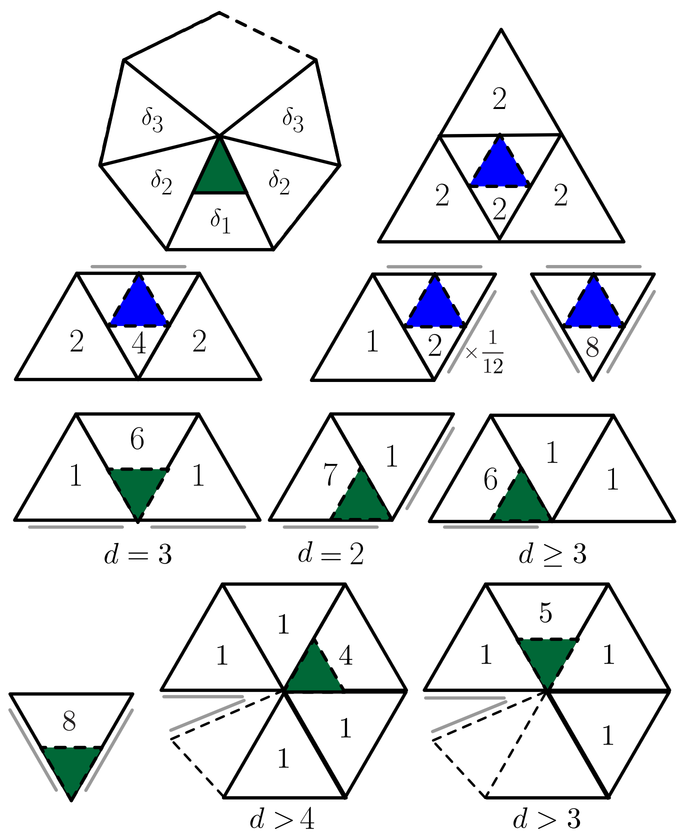

Fig. 2. Modified half-box splines subdivision operator $S_{\mathcal{F}^*}$. Multiply all factors by 1/32 except the δ_i factors or where explicitly stated otherwise. Double edges (with gray) denote boundary edges.

XXXX-XXXX/2020/6-ART1 $15.00
https://doi.org/10.1145/nnnnnnn.nnnnnnn

where β is the halfbox spline parameter, given by

$$\beta = \begin{cases} \frac{1}{12} & d = 3 \\ \frac{1}{8} & d = 4 \\ \frac{1}{4} - \frac{1}{16}\sin^2\left(\frac{2\pi}{5}\right) & d = 5 \\ \frac{1}{4} & \text{otherwise} \end{cases} \tag{5}$$

3 1-FORM SUBDIVISION OPERATOR

For completeness, we list the coefficients for the interior stencils of the S_1 subdivision operator, as used in deGoes et al. [de Goes et al. 2016].

$$\eta_0 = \frac{3}{8} - \alpha - \frac{\beta}{4} \tag{6}$$

$$\eta_1 = \eta_{d-1} = \begin{cases} \frac{1}{8} - \alpha + \frac{\beta}{8} & d = 3, \\ \frac{1}{8} - \alpha & \text{otherwise} \end{cases} \tag{7}$$

$$\eta_2 = \eta_{d-2} = \begin{cases} \frac{\beta}{4} - \alpha & d = 4, \\ \frac{\beta}{8} - \alpha & \text{otherwise} \end{cases} \tag{8}$$

$$\eta_i = -\alpha \quad \text{for } 2 < i < d-2 \tag{9}$$

$$\theta_0 = -\theta_{d-1} = -\frac{\beta}{8} \tag{10}$$

$$\theta_1 = -\theta_{d-2} = \begin{cases} 0 & d = 3, \\ -\frac{\beta}{8} & \text{otherwise} \end{cases} \tag{11}$$

with α, β the coeffficents for Loop resp. halfbox spline subdivision, as defined before.

4 STENCIL CONSTRAINTS

The subdivision operators were created with mirror symmetric templates about the target mesh element. The following commutation relations were imposed

$$\begin{aligned} d_0 S_{\mathcal{V}} &= S_1 d_1 \\ S_{\mathcal{F}^*} d_1 &= d_1 S_1 \\ S_{\mathcal{F}^*} A_{\mathcal{E}^* \to \mathcal{F}^*} &= A_{\mathcal{E}^* \to \mathcal{F}^*} S^*_{\mathcal{E}} \\ C_\Gamma S_\Gamma &= S_{\mathcal{E}^*} C_\Gamma \end{aligned}$$

4.1 Interior stencils of $S_{\mathcal{E}^*}$

For constructing the interior stencils of $S_{\mathcal{E}^*}$, we assume that the stencil coefficients are mirror-symmetric with respect to the subdivided edge element. In addition, as in [Wang et al. 2006], we fix the odd stencil for $S_{\mathcal{E}^*}$ with the same global shape as the S_1 odd stencil. Finally, we demand that the coefficients for even stencils of valence ≥ 7 are the same over the finite support of $S_{\mathcal{F}^*}$.

After construction of the new $S_{\mathcal{E}^*}$ operator via the commutations, there are three degrees of freedom remaining. We resolve two of them by requiring all coefficients of the even valence 6 stencil to be positive. The remaining degree of freedom is present in the valence 4 even stencil, for which the local subdivision operator spectrum is $[1/4, 3/16, 3/16, 1/8, 1/8, 1/8, 1/16, 3/16 - 4z]$, where z is the remaining degree of freedom. We choose $z = 1/32$ to make the spectrum consist of $1 \times 1/4, 2\times, 3/16, 3 \times 1/8, 2 \times 1/16$.

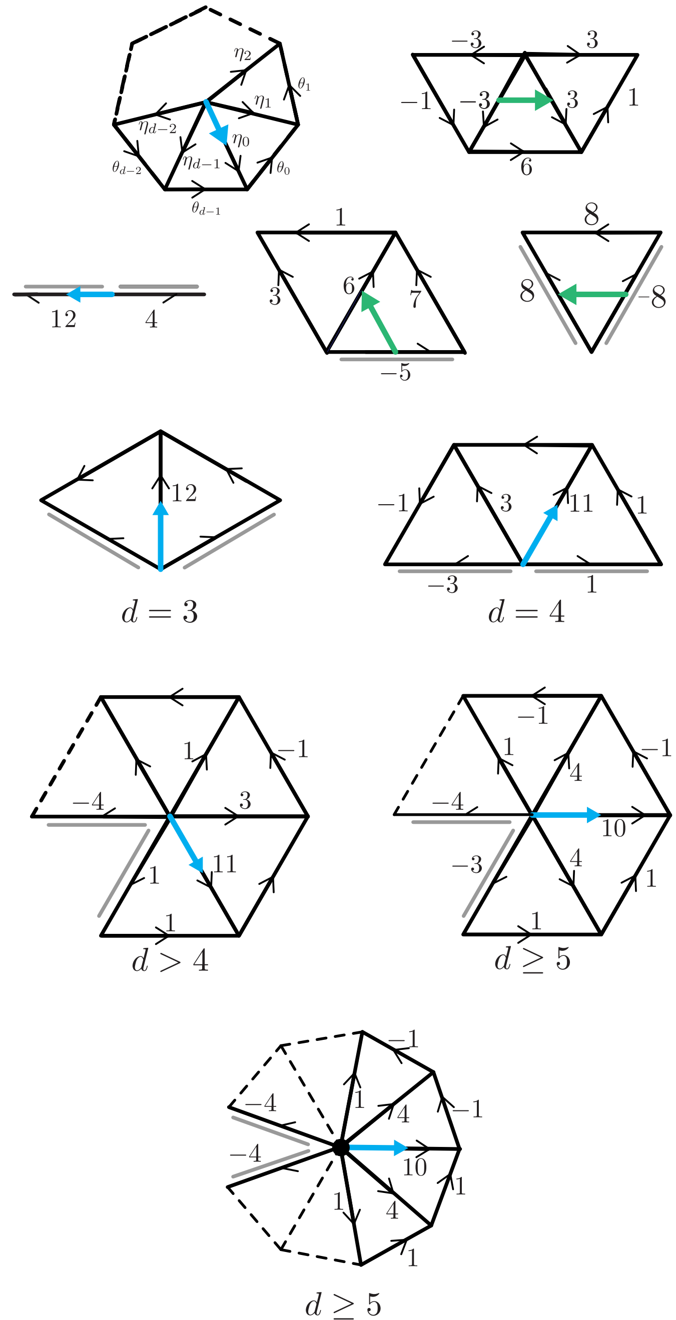

Fig. 3. 1-form subdivision operator S_1. Arrows denote assumed edge direction. Multiply all factors by 1/32 except for the η_i, θ_i factors. In the bottommost stencil, when the boundary edge and the first edge of the interior stencil coincide, the coefficients should be summed up together. Similar goes for the odd interior stencil for valence 3.

The stencils of the $S_{\mathcal{E}^*}$ operator are summarized in Figure 4. The coefficients ζ and ζ' for the valence 5 interior rings are given by

$$\zeta = \frac{2}{\sqrt{5}+5}, \zeta' = 1 - \zeta \tag{12}$$

5 BOUNDARY STENCILS

We assume all boundary stencils to be applied with mirror symmetry around the boundary. Since we want to preserve the $C\gamma = 0$ condition on the boundary, we demand that the coefficients for the boundary stencil for even elements of $S_{\mathcal{E}^*}$ solely depend on the boundary. In addition, we require that the odd stencil for the elements that touch the boundary with one of their vertices remains the same for $d \geq 3$. Using these assumptions on the stencils, we solve for $S_{\mathcal{E}^*}$, $S_{\mathcal{F}^*}$ and S_1 in conjunction. The resulting subdivision operators have a single degree of freedom left, which we resolve by requiring all $S_{\mathcal{F}^*}$ elements to be positive. The modified stencils for $S_{\mathcal{F}^*}$ are shown in Figure 2, for S_1 in Figure 3, and for $S_{\mathcal{E}^*}$ in Figure 4.

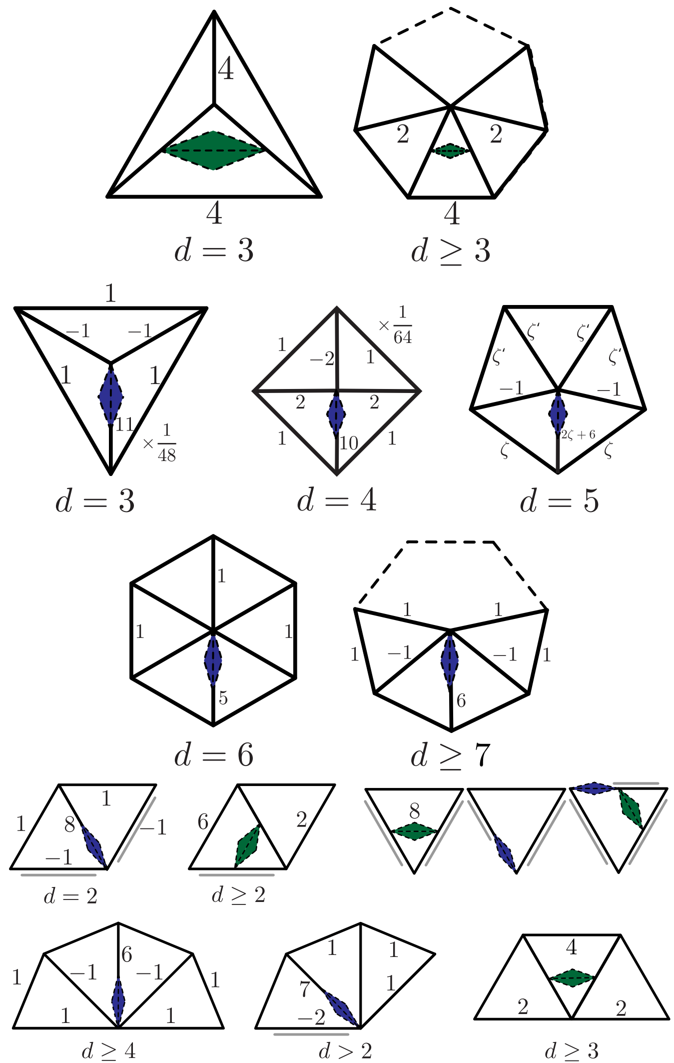

Fig. 4. Unsigned integrated edge subdivision $S_{\mathcal{E}^*}$. Multiply all factors by 1/32 unless stated otherwise. Double edges denote boundary edges. When the outer edges with coefficients of the interior odd stencil coincide for valence 3, sum the coefficients.

REFERENCES

Henning Biermann, Adi Levin, and Denis Zorin. 2000. Piecewise Smooth Subdivision Surfaces with Normal Control. In *Proceedings of the 27th Annual Conference on Computer Graphics and Interactive Techniques (SIGGRAPH '00)*. ACM Press/Addison-Wesley Publishing Co., New York, NY, USA, 113–120. https://doi.org/10.1145/344779.344841

Fernando de Goes, Mathieu Desbrun, Mark Meyer, and Tony DeRose. 2016. Subdivision Exterior Calculus for Geometry Processing. *ACM Trans. Graph.* 35, 4, Article 133 (July 2016), 11 pages. https://doi.org/10.1145/2897824.2925880

Ke Wang, Yiying Tong, Mathieu Desbrun, Peter Schröder, et al. 2006. Edge subdivision schemes and the construction of smooth vector fields. *ACM Transactions on Graphics* 25, 3 (2006).